Multilayer thin film design for far ultraviolet polarizers using an induced transmission and absorption technique

Jongmin Kim, Muamer Zukic, and Douglas G. Torr

Department of Physics, The University of Alabama in Huntsville
Optics Building, Suite 300, Huntsville, AL. 35899

Abstract

An explanation of induced transmission for spectral regions excluding the far ultraviolet (FUV) is given to better understand how induced transmission and absorption can be used to design effective polarizers in the FUV spectral region. We achieve high s-polarization reflectance and a high degree of polarization [P=(Rs-Rp)/(Rs+Rp)] by means of a MgF_2/Al/MgF_2 three layer structure on an opaque thick film of Al as the substrate. For example, our polarizer designed for the Lyman-α line (λ=121.6 nm) has 87.95% reflectance for the s-polarization case, and 0.43% for the p-polarization case, with a degree of polarization of 99.03%. If a double reflection polarizer is made with this design, it will have a degree of polarization of 99.99% and s-polarization throughput of 77.35%.

Key words : thin film, polarizer, FUV, filter, transmission

(to be submitted to Optical Engineering)

1. Introduction

In the far ultraviolet (FUV) region, a MgF_2 crystal is known to be birefringent down to 130 nm.[1] Johnson[2] reported a MgF_2 transmission polarizer with 40% transmittance down to 160 nm which then dropped to zero near 120 nm. Winter and Ortjohann[3] used a 'pile-of-plates' transmission polarizer made of four MgF_2 crystal plates for the Lyman-α line (λ=121.6 nm). The transmittance was 20% and the degree of polarization was 85±1 %.

Mallrath[4] and Saito et. al.[5] used a LiF crystal as a reflection polarizer. Also, Hass and Hunter[6] found that a MgF_2 crystal worked well as a reflection polarizer. Complete polarization can be achieved when a crystal is oriented at its Brewster angle. However, metal surfaces have much higher reflectances than crystals. The reflectance curves for a metal are very similar to those obtained from a dielectric in the visible region, with the exception that the metallic reflectance is generally greater and the minimum reflectance of the p-polarization does not go to zero as in the case of a dielectric. Hunter[7] showed that for optimum polarization, n, the index of refraction, should be large and k, the extinction coefficient, should be small. Therefore, when the optimum polarization is obtained, the reflectance is low.

A single metal surface at the Pseudo-Brewster angle of incidence is not enough for a high degree of polarization. Hamm et. al.[8] designed a triple-reflection-polarizer (TRP) using gold coated mirrors. Because it had a high polarization ratio (Rs/Rp ~ 19) and maintained the direction of incident radiation, it was used by several authors.[9~11] The transmittance of the unpolarized light of such a system was about 4%. The merit of the metal multi-surface polarizer is that it works well in a broad wavelength region.

In contrast to the single metallic surface, a thin film multilayer can provide the freedom to specify the incident angle. We report multilayer polarizer designs which have a higher degree of polarization and a higher s-polarization reflectance than the metal surface polarizer. We design the polarizer by inducing absorbed and transmitted p-polarized light. We optimize the design for specific FUV emission lines and a 45° angle of incidence for the convenience of experimental setup.

2. Induced transmission technique

Long ago, Berning and Turner[12] showed that a reasonably thick metal film can be induced to transmit a suprising amount of energy of a particular wavelength when it is surrounded by suitably chosen interference film combinations. They called this technique 'induced transmission (IT)' and explained a mathematical step to achieve IT to design a narrow band pass filter. Because the performance of IT filters has some useful advantages - the freedom from sidebands and relatively rapid transitions between pass band and stop band - many authors[13-21] have tried to improve the design steps. Kard[13] used simplified Vlasov formulas, Landau and Lissberger[14] used equivalent layer method, and Holloway and Lissberger[15] used the effective interface method. Graphical tools were also used. Berning and Turner[12] used a circle diagram chart and Baumeister et. al.[16] used a parametric admittance plot. All these authors succeed to find IT designs but their design procedures were very complicated. This is because the physical mechanism of IT has not been fully understood.

Figure 1 shows the basic structure of an IT filter with one metal layer. It consists of a high absorbing center metal layer and a dielectric stack on both sides of the metal layer. Each dielectric stack has several (5~6) layers of high and low quarterwave stack and a phase adjusting layer. The phase adjusting layers are located next to the center metal layer, so that the total structure is symmetric. The

authors considered normal incidence and the incident media were the same as the substrates. Some of authors also considered other structures which contained two metal layers. But their performances were worse than the those filters with one metal layer and we do not consider them here.

Figure 2 shows the top half of an IT filter which was designed by Berning and Turner.[12] It also shows the phase changes for some of the reflected rays at each boundary. The lights reflected from the first 6 boundaries are in phase with each other but the light reflected from the 7 th boundary is almost (not exactly) out of phase with the others. When we add or substract the number of quarterwave stack layers, keeping all other parameters the same (symmetricity, thicknesses of the phase adjusting layers and metal layer), the transmittance drops dramatically. The reflection at the last boundary is much higher compared to the other boundaries and the ray reflected from this boundary should be designed to interfere destructively with the other rays reflected from the quarterwave stack boundaries. Therefore, the quarterwave stack is needed for compensation of the rays from the high reflecting metal surface by reflecting rays of similar amplitude which are out of phase.

If we consider the center Ag layer as a substrate (there is no light coming from the bottom of Ag layer), the maximum transmittance into the Ag layer is obtained when the phase adjusting layer has a thickness which makes reflection from Ag boundary exact out of phase with the others.(We call this thickness as $d_{P.A.}{}^{o}$) We examine the change of two phase adjusting layer thicknesses which give the best IT performance for different Ag layer thicknesses in Berning and Turner's design. Whenever the best transmittance is obtained for different Ag layer thicknesses, the top and bottom phase adjusting layers have the same thickness. Figure 3 shows the change of the best thickness of the phase adjusting layers as a function of Ag layer thickness. It shows that as the Ag layer is getting thinner - more light can come back from the bottom of Ag layer - the thickness of phase adjusting layer($d_{P.A.}$) is farther from the thickness $d_{A.P.}{}^{o}$. Therefore, it is obvious that the phase adjusting layer plays an important role in the out of phase relation between reflected light including the light coming from the bottom of the Ag layer. Because of the strong absorption of the Ag layer, the light coming from the bottom of Ag layer is weak and $d_{P.A.}$ is very close to $d_{P.A.}{}^{o}$.

The dielectric stack below the central Ag layer, which is symmetric to the top dielectric stack, is explained by considering the IT filter structure as a Fabry-Perot etalon. When a spacer layer has absorbing properties the transmittance of a Fabry-Perot etalon is given by

$$T = \frac{|t_{12}|^2 |t_{23}|^2 e^{\frac{4\pi}{\lambda} k_{Ag} d_{Ag}}}{1 + |r_{21}|^2 |r_{23}|^2 e^{\frac{8\pi}{\lambda} k_{Ag} d_{Ag}} - 2e^{\frac{4\pi}{\lambda} k_{Ag} d_{Ag}} \mathrm{Re}(r_{21} r_{23} e^{-i\frac{4\pi}{\lambda} n_{Ag} d_{Ag}})} \qquad (1)$$

for normal incidence. Here t and r are amplitude transmittance and reflectance and subscripts 1, 2, and 3 represent incident, spacer, and substrate mediums, respectively. λ is the design wavelength and d_{Ag} is the physical thickness of the Ag(spacer) layer. Re is the real part of a complex number. Using a reversibility relation of the transmittance

$$\mathrm{Re}\left(\frac{n_{Ag}+ik_{Ag}}{n_1}\right)|t_{12}|^2 = \mathrm{Re}\left(\frac{n_1}{n_{Ag}+ik_{Ag}}\right)|t_{21}|^2 \qquad (2)$$

we can replace $|t_{12}|^2$ in Eq. (1) with

$$|t_{12}|^2 = \frac{n_1^2}{n_{Ag}^2 + k_{Ag}^2}|t_{21}|^2 \qquad (3)$$

Then Eq.(1) is a function of t_{21}, t_{23}, r_{21}, and r_{23}. For an IT filter of which the incident medium (1) is same as the substrate (3), there can be only one set of t_{21} (=t_{23}) and r_{21} (=r_{23}) that gives best transmission T for a specific n_1 (=n_3), n_{Ag}, k_{Ag}, and d_{Ag}. Therefore, whenever the incident medium is the same as the substrate medium and the top dielectric stack is designed properly, the symmetric structure gives the best IT performance.

The top dielectric stack is used to make the light interfere constructively when it enters the center Ag layer. Likewise, the bottom dielectric makes the light interfere constructively when it enters the substrate. Therefore, IT is obtained by minimizing the reflectance. As a result, the IT structure has maximum absorptance for the passband wavelengths.

From this point of view, we can simplify the IT filter design procedure.
After the coating materials are decided,

1) Assuming a metal layer as a substrate, calculate the thickness of the phase adjusting layer to achieve destructive interference between reflected waves.
2) Decide the number of dielectric quarterwave layers to maximize the transmittance into the metal substrate.
3) Select the thickness of the metal layer : as the metal layer is getting thicker the signal is lowered. As the metal layer is getting thinner, the background is increased.
4) Put the same dielectric structure in reverse order below the metal layer.
5) Adjust the thicknesses of the two phase adjusting layers to give the best IT performance.

Using a personnel computer this procedure can be followed easily without the use of any complex formulas or complicate graphical methods.

3. Design of an FUV multilayer polarizer

As we explained in a previous section, IT is obtained by minimizing the reflectance. We use this concept to design a reflection FUV polarizer. For an oblique angle of incidence reflected and transmitted light are different for s- and p-polarizations. If we make the p-polarization reflectance very small maintaining a large s-polarization reflectance, the reflector works as a polarizer.

To achieve this reflectance difference we use the boundaries between the high and low absorbing materials. The Fresnel coefficients are complex numbers for absorbing film materials. Amplitude changes as well as phase angle changes are different between the two polarizations. The differences are large at the boundary between high and low absorbing materials. LiF is the lowest absorbing material in the FUV region, but it is hygroscopic and has been proved unsuitable for applications in a high energy radiation environment. MgF_2 is the most attractive low absorbing material in this region. Al is chosen as the high absorbing material because it is the only material that has a high reflectance down in this short wavelength range.

In the FUV region, even MgF_2 exhibits absorption and we cannot make use of a quarterwave stack as in IT filters. We must minimize the number of layers to achieve a high reflectance of s-polarization. Therefore, a MgF_2/Al/MgF_2 three layer stack on a thick opaque Al substrate is examined.

For an estimation of the film thicknesses, we use the method of summation.[22] In analyzing a multilayer thin film, this summation method is more straightforward than the matrix methods. Using this method we can trace step by step every reflected and transmitted wave, and select important waves among all the multiply reflected waves. Important waves are those which have much larger amplitudes than other waves at a specific point. Considering the phase difference between important waves, we estimate the thin film thickness.

Figure 4 shows the light waves we consider to determine the thin film thicknesses. Table 1 shows the Fresnel reflection and transmission coefficients for the p-polarization state and 121.6 nm when the light is incident at a 45° angle of incidence. We use optical constants of Al and MgF_2 from reference 23 and 24, respectively.

The role of the top MgF_2 layer is to maximize the amount of the p-polarized light that can pass through the center Al layer. In the IT filter case this role is accomplished by making the reflected light interfere destructively. For our polarizer case, the transmission of the p-polarized light is maximized by making the reflected light interfere constructively. This is because we have only two boundaries above the center Al layer and the amplitudes of the Fresnel reflection coefficients are quite different between these two boundaries. This is explained in Figure 5. Figure 5-(a) shows the case when we make the reflected light from the first two boundaries interfere destructively (a and b in Figure 4). Then the electric fields that reach the second boundary can interfere constructively (c and d in Figure 4), and this gives a large reflected amplitude from that boundary (b in Figure 4). Even though this light interferes destructively with the light reflected from the first boundary (a in Figure 4), the result is still a large reflectance. Figure 5-(b) shows the opposite case. In this case, the top MgF_2 layer is designed for constructive interference between the reflected waves and also the electric fields that reach the second boundary interfere destructively. There is also a small reflectance from the 2nd boundary. This reflected light interfere constructively with the light reflected from the first boundary, the sum is smaller than in case (a). In Figure 4 the wave d passes through the top MgF_2 layer twice, and is reflected at the first and second boundary after it starts from c. The thickness of the top MgF_2 layer is determined to make the sum of the phase changes of this round trip equal to π.

In the IT filter bottom dielectric stack is used for the same purpose as the top one. For the polarizer, we use the fact that the MgF_2 layer is sandwiched by high reflecting Al layers. This bottom MgF_2 layer is designed for use as a transmission and absorption induced layer for p-polarization. In order to induce absorption, the sum of the waves going up to the central Al layer must have a large amplitude.

This is achieved by making the waves interfere constructively. For this purpose, we consider the f and g waves as important waves in Figure 4. The amplitudes of the transmission coefficient are 1.16 and 1.35 at the Al/MgF_2 and MgF_2/Al boundaries, respectively. The reflection coefficient at the MgF_2/Al boundary is 0.96. The decrease in amplitude by propagation through the MgF_2 layer is small. Therefore, f and g have larger amplitudes than e, in Figure 4. Furthermore, the multiply reflected waves h — can be made in phase with f and g. For the transmission induced layer, i and j waves are important. If we make them interfere constructively, they will have large amplitudes when they go into the substrate. As a result, this three layer structure has a large transmittance for p-polarization. The constructive interference between f and g and between i and j are achieved simultaneously, because the bottom MgF_2 layer is sandwiched by Al. The phase differences between f and g, and i and j are equal. The thickness of the bottom MgF_2 layer is chosen to make the phase difference equal to zero. Consequently, the bottom MgF_2 layer thickness is approximately half that of the top MgF_2 layer.

The exact thicknesses of the two MgF_2 layers and the best thickness of the central Al layer are determined by computer fitting. Figure 6 shows the changes of the electric field in one of our polarizers designed for the Lyman-α line at a 45° angle of incidence. The electric waves at the top and bottom of each boundary in the three layer thin film are calculated by the method explained in reference 25. In the figure, the length and the direction of the line are the amplitude and the phase angle of the electric field relative to the incident wave. Because we consider the tangential components for both polarizations, the sum of the fields are continuous at every boundary. This shows that with the help of the top MgF_2 layer, most of the p-polarized waves pass through the high absorbing Al layer. It also shows that the bottom MgF_2 layer works as a transmission and absorption induced layer. Due to the differences in the Fresnel coefficients between the two polarizations at oblique angle of incidence, we achieve a good reflection polarizer. For this design, the s-polarization has 0.97% transmittance and 10.36% absorptance.

4. Results

Figure 7 shows one of the calculated results designed for the Lyman-α line at a 45° angle of incidence. The design has a 87.95% reflectance for the s-polarization case, and a 0.43% reflectance for the p-polarization case. The degree of polarization P=(Rs-Rp)/(Rs+Rp) is 99.03%. If we make a double reflection polarizer with this design, a 99.99% degree of polarization with a 77.35% s-polarization reflectance is achieved. The spectral distribution of the degree of polarization for the single, double and triple reflection polarizers, respectively, are shown in Figure 8. A four reflection polarizer can even made which does not change the direction of the incident light. The four reflection polarizer has 59.83 % s-polarization reflectance, and a degree of polarization very close to 100%.

Utilizing the same approach, we can design the three layer structure for any wavelength in the FUV region. A polarizer designed for 130.4 nm and a 45° angle of incidence is shown in Figure 9. It has a 92.74% s-polarization reflectance and a 0.001% p-polarization reflectance. As a single reflection polarizer, the degree of polarization is almost 100%. Another polarizer for the 135.6 nm line at the same angle of incidence has a 93.01% s-polarization reflectance and a 0.005% p-polarization reflectance. It has a 99.99% degree of polarization as a single reflection polarizer.

The next step in our research is to fabricate and characterize FUV polarizers. The problems in fabricating the Al layers and our plans to solve them were reported in reference 26. The final results will be reported later.

5. Summary

We explain the concept of induced transmission from a physical point of view. Based upon this new knowledge, we use a concept of induced transmission and absorption to design a multilayer reflection polarizer in the FUV region. Using MgF_2 and Al as low absorbing and high absorbing materials pair, we achieve high s-polarization reflectance and a high degree of polarization. For example, a polarizer designed at the Lyman-α line at a 45° angle of incidence has 87.95% reflectance for s-polarization and 0.43% reflectance for p-polarization. The degree of polarization of this design is 99.03% as a single reflection polarizer and 99.99% as a double reflection polarizer. For the 130.4 nm line and a 45° angle of incidence, our design has a 92.74% s-polarization reflectance and a 0.001% p-polarization reflectance with almost a 100% degree of polarization. Another design for 135.6 nm at the same angle of incidence has 93.01% and 0.005% reflectances for s- and p-polarizations, respectively, with a 99.99% degree of polarization. Our polarizers are designed for a 45 angle of incidence, but any other angle can be selected if needed.

6. Acknowledgements

This work was supported by NASA contract NAS8-38145, NASA grant NAGW-2898. The first author would like to thank the Agency for Defense Development of Korea and the Physics Department of the University of Alabama in Huntsville for the graduate student assistantship received during this study.

7. References

1. J. A. R. Samson, *Techniques of Vacuum Ultraviolet Spectroscopy*, pp. 296-319, John Wiley & sons., New York, (1967).
2. W. C. Johnson, "Magnesium fluoride polarizing prism for the vacuum ultraviolet", *Rev. Sci. Instrum.* 35, 1375, (1964).
3. H. Winter and H. W. Ortjohann, "High transmission polarization analyzer for Lyman-α radiation", *Rev. Sci. Instrum.*, 58, 359, (1987).
4. T. J. McIlrath, "Circular polarizer for Lyman-α flux", *J. Opt. Soc. Am.*, 58, pp. 506, (1968).
5. T. Saito, A. Ejiri, and H. Onuki, "Polarization properties of an evaporated aluminum mirror in the VUV region", *Appl. Opt.* 29, 4538, (1990).
6. G. Hass and W. R. Hunter, "Reflection polarizers for the vacuum ultraviolet using Al + MgF_2 mirrors and MgF_2 plate", *Appl. Opt.* 17, 76, (1978).
7. W. R. Hunter, "Polarizers for the extreme ultraviolet", *Jpn. J. Appl. Phys.*, 4(Supp. 1), 520, (1965).
8. R. N. Hamm, R. A. MacRae, and E. T. Arakawa, "Polarization studies in vacuum ultraviolet", *J. Opt. Soc. Am.* 55, 1460, (1965).
9. I. C. Malcolm, H. W. Dassen, and J. W. McConkey, "Polarization of radiation from H_2 excited by electron impact : Lyman and Werner emissions and Lyamn-α", *J. Phys. B:Atom. Molec. Phys.* 12, 1003, (1979).
10. P. Zetner, A. Pradhan, W. B. Westerveld, and J. W. McConkey, "Polarization analysis techniques in the VUV", *Appl. Opt.* 22, 2210, (1983).

11. W. B. Westerveld, K. Becker, P. W. Zetner, J. J. Corr, and J. W. McConkey, "Production and measurement of circular polarization in VUV", *Appl. Opt.*, 24, 2256. (1985).
12. P. H. Berning and A. F. Turner, "Induced transmission in absorbing films applied to band pass filter design", *J. Opt. Soc. Am.* 47(3), 230-239 (1957).
13. P. G. Kard, "Theory of Increasing the transparency of metallic coatings", *Opt. Spectrosc.* 9, 129-131 (1960).
14. B. V. Landau and P. H. Lissberger, "Theory of Induced-Transmission Filters in Terms of the Concept of Equivalent Layers", *J. Opt. Soc. Am.* 62(11), 1258-1264 (1972).
15. R. J. Holloway and P. H. Lissberger, "The Design and Preparation of Induced Transmission Filters", *Appl. Opt.* 8(3), 653-660 (1969).
16. P. W. Baumeister, V. R. Costish, and S. C. Pipper, "Bandpass Filters for the Ultraviolet", *Appl. Opt.* 4(8), 911-914 (1965).
17. P. H. Lissberger, "Coatings with induced transmission", *Appl. Opt.* 20(1), 95-104 (1981).
18. P. W. Baumeister, "Padient Power Flow and Absorptance in Thin Films", *Appl. Opt.* 8(2), 423-436(1969).
19. D. J. Hemingway and P. H. Lissberger, "Properties of weakly absorbing multilayer systems in terms of the concept of potential transmittance", *Optica Acta* 20(2), 85-96 (1973).
20. A. Thetford, "Absorbing multilayers and reflection interference filters", *Optica Acta* 25(10), 945-961 (1978).
21. S. Yang, "Circular, variable, broad-bandpass filters with induced transmission at 200-1100nm", *Appl. Opt.* 32(25), 4836-4842 (1993).
22. O. S. Heavens, *Optical Properties of Thin Solid Films*, 55-59, Dover, New York, (1965).
23. Y. D. Smith, E. Shiles, and M, Inokuti, "The optical properties of metallic aluminum", in *Handbook of Optical Constants of Solids*, E. D. Palik Ed., pp. 369-406, Academic Press, Orlando, (1985).
24. M. Zukic, D. G. Torr, J. F. Spann, and M. R. Torr, "Vacuum ultraviolet thin films 1: Optical constants of BaF_2, CaF_2, LaF_3, MgF_2, Al_2O_3, HfO_2, and SiO_2 thin films", *Appl. Opt.* 29(28), 4284- 4292(1990).
25. J. Kim, M. Zukic, D. G. Torr, and M. M. Wilson, "Multilayer thin film design as far ultraviolet quarterwave retarders", *Multilayer and Grazing Incidence X-Ray/EUV Optics for Astronomy and Projection Lithography*, R. B. Hoover and A. B. C. Walker Jr. ed., Proc. SPIE, 1742, 403-412, (1992).
26. J. Kim, M. Zukic, M. M. Wilson and D. G. Torr, "Design and Fabrication of Reflection Far Ultraviolet Polarizers and Retarders", *X-Ray and Ultraviolet Polarimetry*, S. Fineschi ed., Proc. SPIE, 2010, (1993). (in press)

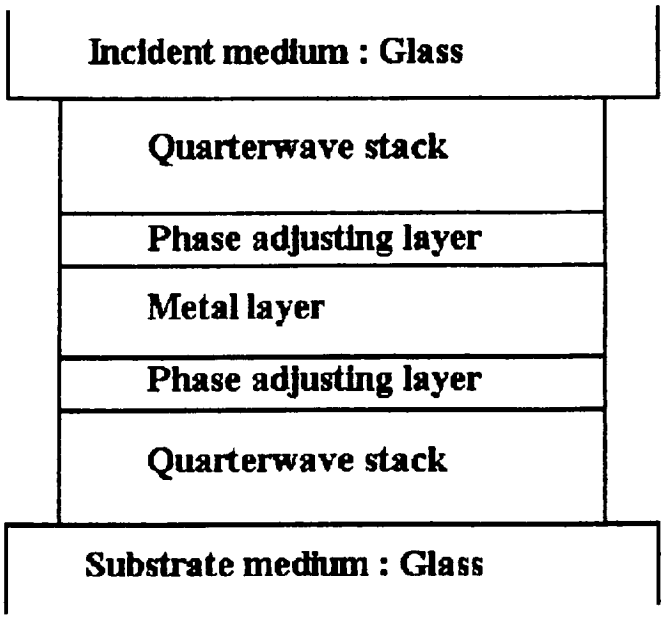

Figure 1. Schematic diagram of the structure of a single metal layer IT filter.

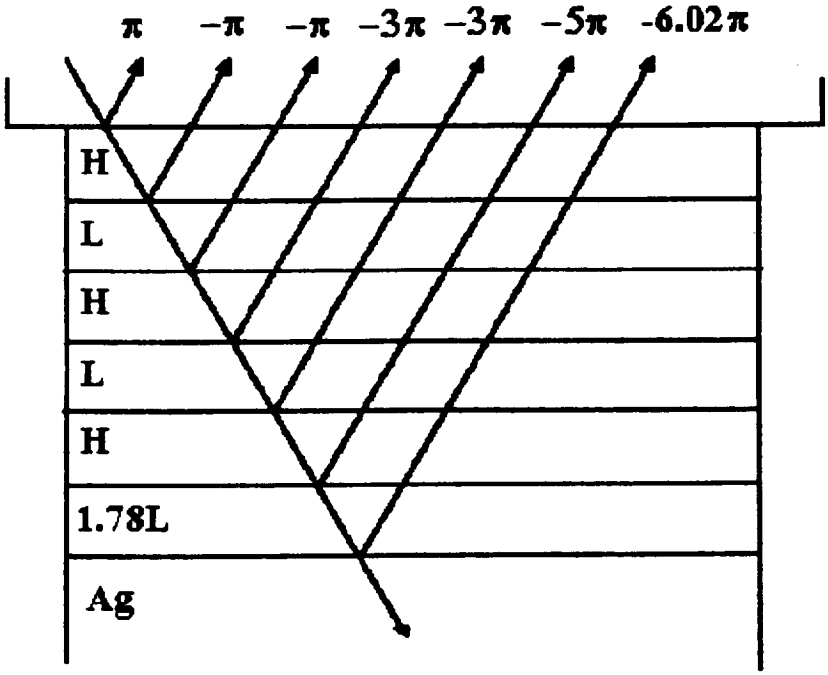

Figure 2. Phase changes of some of the reflected rays for the upper half of an IT filter designed by Berning and Turner.

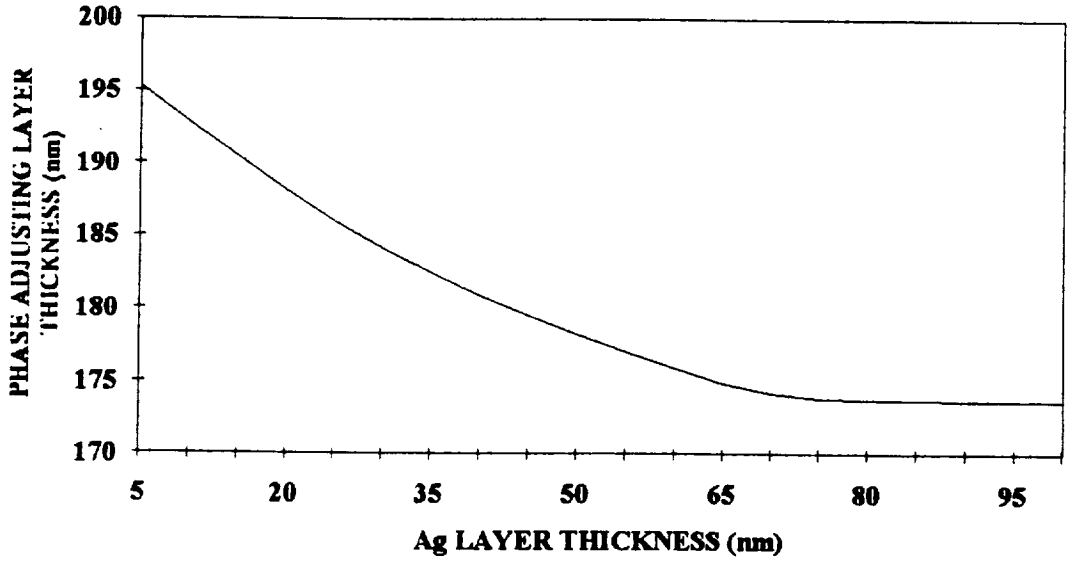

Figure 3. Change of the phase adjusting layer thickness as the Ag layer thickness changes in Berning and Turner's IT filter. In this specific deisgn $d_{P.A.}{}^{\circ}$ corresponds to 173.6 nm.

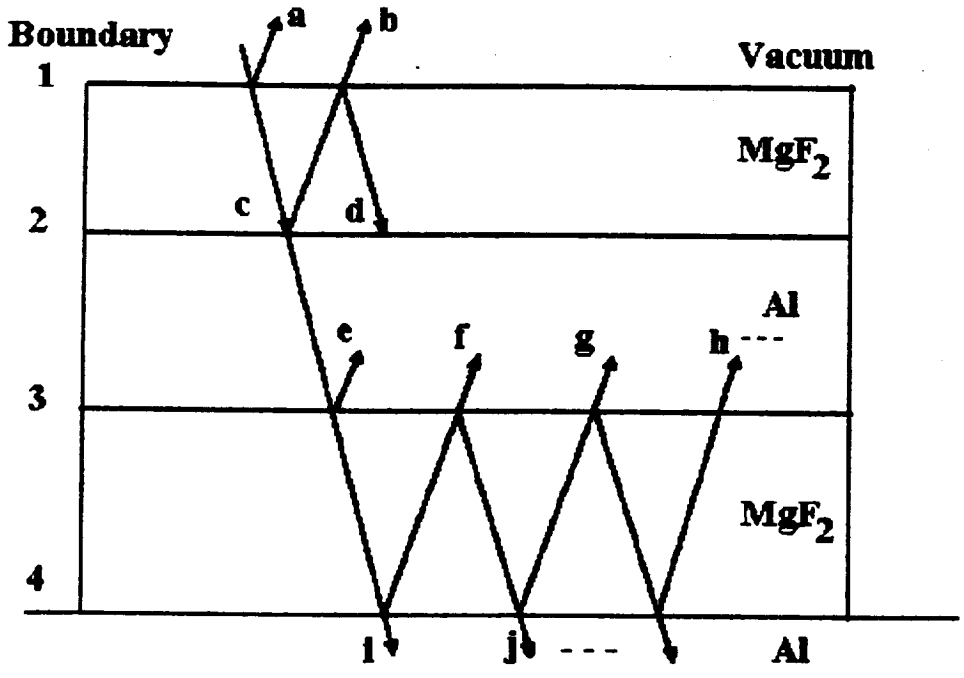

Figure 4. Important light waves for estimation of the thickness of the MgF_2 layers.

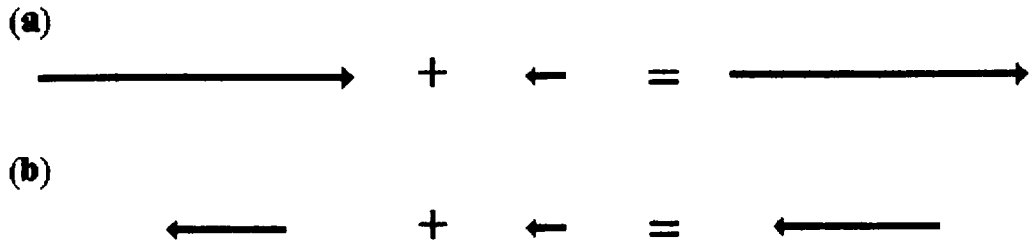

Figure 5. Two different phase relations between reflected waves from vacuum/MgF_2 and MgF_2/Al boundaries.

(a) distructive interference

(b) constructive interference

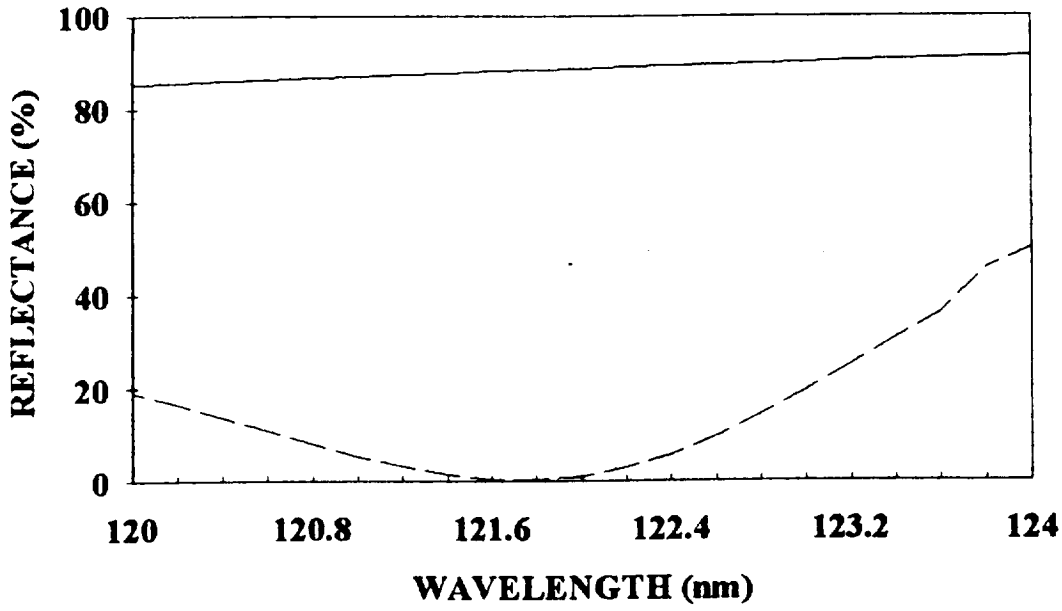

Figure 7. Calculated reflectances for s-polarization (solid line) and p-polarization (dashed line) of a polarizer designed for the Lyman-α line at a 45° angle of incidence.

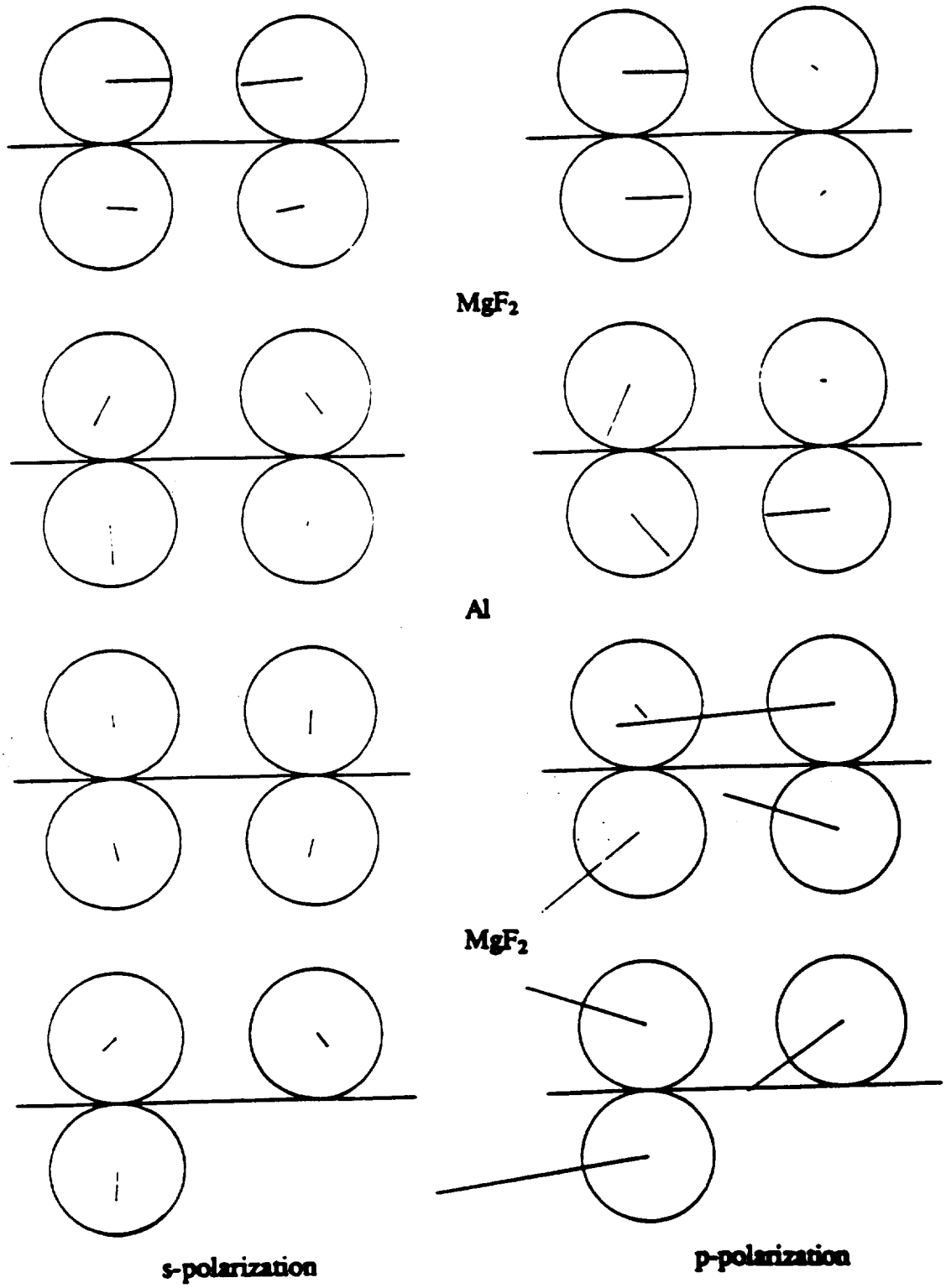

Figure6. Incoming and outgoing electric fields at the top and bottom of each boundary for the 121.6 nm polarizer case for the s- and p-polarization respectively. The left hand side is the incoming wave and the right hand side is the outgoing wave for each polarization.

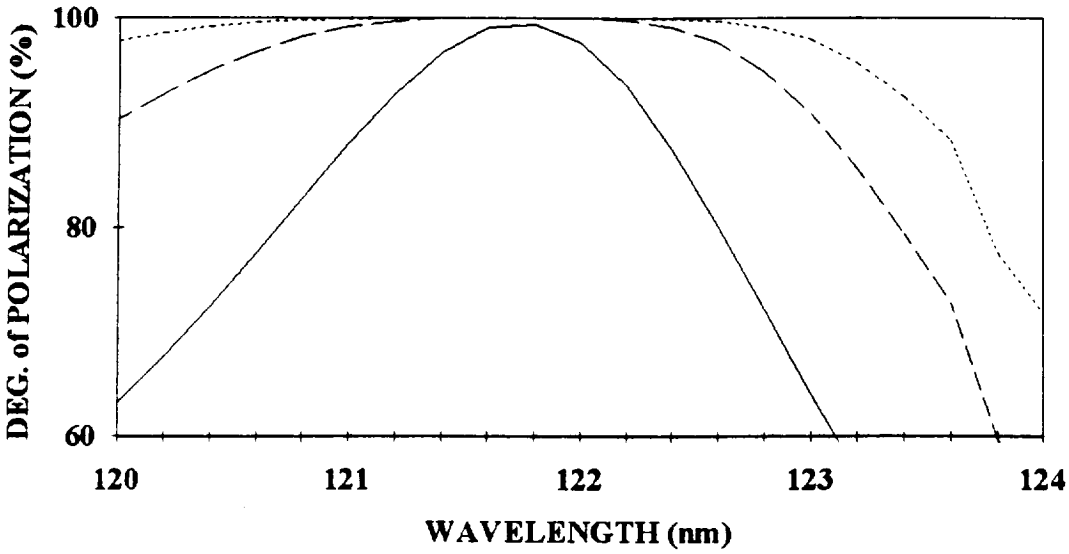

Figure 8. Calculated degrees of polarization for the single (solid line), double (dashed line), and triple (dotted line) reflection polarizer made of the design shown in Figure 7.

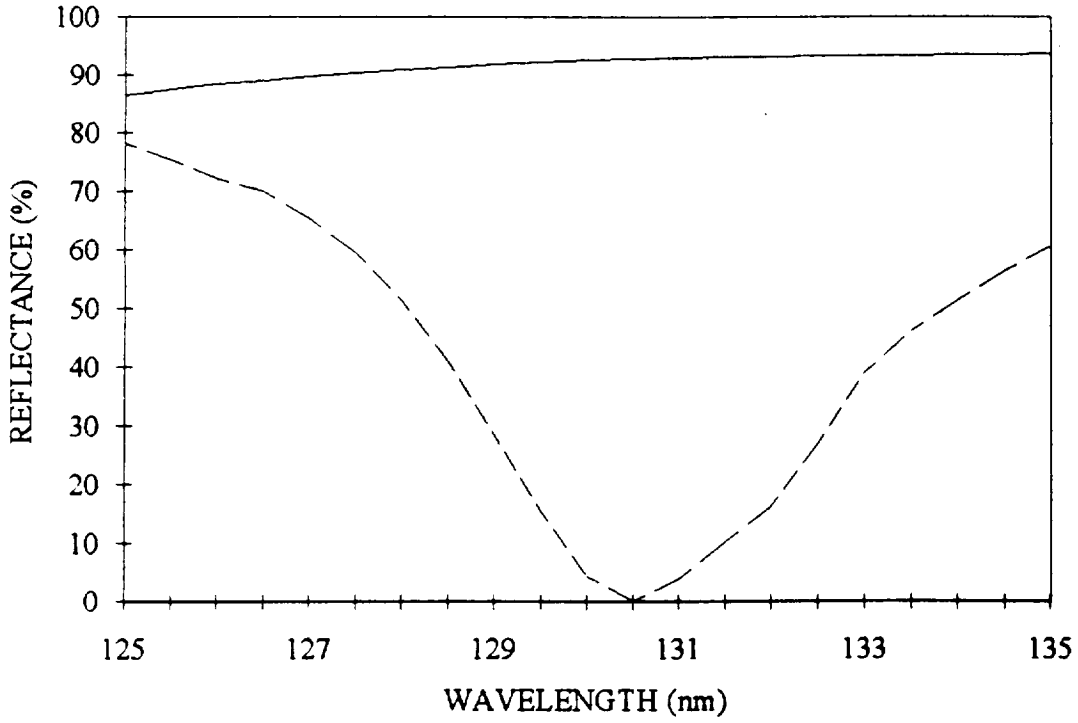

Figure 9. Calculated reflectances for s-polarization (solid line) and p-polarization (dashed line) of a polarizer designed for 130.4 nm at a 45° angle of incidence.

Incident	Reflection at Boundary			Transmission at Boundary		
Material	Vacuum	MgF2	Al	Vacuum	MgF2	Al
Vacuum		0.14			0.67	
		(+178.6)			(+0.3)	
MgF2	0.14		0.96	1.47		1.35
	(-1.4)		(+54.5)	(-0.3)		(+27.1)
Al		0.96			1.16	
		(-125.5)			(-60.8)	

Table 1. The Fresnel reflection and transmission coefficients for p-polarization light incident at a 45 angle of incidence from vacuum. top : amplitude ratio of the reflected or ransmitted light to the incident light. (bottom): phase angle change.